
COLONFORMER: AN EFFICIENT TRANSFORMER BASED METHOD FOR COLON POLYP SEGMENTATION

A PREPRINT

Nguyen Thanh Duc

School of Information and Communication Technology
Hanoi University of Science and Technology
duc.nt170058@sis.hust.edu.vn

Nguyen Thi Oanh

School of Information and Communication Technology
Hanoi University of Science and Technology
oanhnt@soict.hust.edu.vn

Nguyen Thi Thuy

Faculty of Infomation Technology
Vietnam National University of Agriculture
ntthuy@vnu.edu.vn

Tran Minh Triet

University of Science
Vietnam National University Ho Chi Minh City
tmtriet@fit.hcmus.edu.vn

Dinh Viet Sang *

School of Information and Communication Technology
Hanoi University of Science and Technology
sangdv@soict.hust.edu.vn

May 18, 2022

ABSTRACT

Identifying polyps is a challenging problem for automatic analysis of endoscopic images in computer-aided clinical support systems. Models based on convolutional networks (CNN), transformers, and combinations of them have been proposed to segment polyps with promising results. However, those approaches have limitations either in modeling the local appearance of the polyps only or lack of multi-level features for spatial dependency in the decoding process. This paper proposes a novel network, namely ColonFormer, to address these limitations. ColonFormer is an encoder-decoder architecture with the capability of modeling long-range semantic information at both encoder and decoder branches. The encoder is a lightweight architecture based on transformers for modeling global semantic relations at multi scales. The decoder is a hierarchical network structure designed for learning multi-level features to enrich feature representation. Besides, a refinement module is added with a new skip connection technique to refine the boundary of polyp objects in the global map for accurate segmentation. Extensive experiments have been conducted on five popular benchmark datasets for polyp segmentation, including Kvasir, CVC-Clinic DB, CVCColonDB, EndoScene, and ETIS. Experimental results show that our ColonFormer achieve state-of-the-art performance on all benchmark datasets.

Keywords Semantic segmentation · Deep learning · Encoder-decoder network · Polyp segmentation · Colonoscopy

1 Introduction

Colorectal cancer (CRC) is among the most common types of cancer worldwide, causing over 694,000 fatalities each year [3]. The most common cause of CRC is colon polyps, particularly adenomas with high-grade dysplasia [13]. According to a longitudinal study [10], every 1% increase in adenoma detection rate is linked to a 3% reduction in the risk of colon cancer. As a result, detecting and removing polyps at an early stage is critical for cancer prevention

*Corresponding author

and treatment. Colonoscopy is regarded as the gold standard for colon screening and is recommended procedure in many different societies' guidelines [22]. Nonetheless, overburdened healthcare systems, particularly in low-resource settings, may result in shorter endoscopy durations and more missed polyps [29, 2]. According to a review of the literature, the proportion of colon polyps missing during endoscopies could range from 20 to 47 percent [30]. As a result, research into developing computer-aided tools to assist endoscopists is critical, both in terms of training and implementation in clinical practice.

Advancements in artificial intelligence and deep learning have changed the landscape of such systems. Attempts have been made to develop computer-aided diagnostic (CAD) systems for the automatic detection and prediction of polyps, which could benefit clinicians in detecting lesions and lower the false detection rate [34, 56, 28]. Deep neural networks have shown great potential in assisting colon polyp detection in a number of retrospective investigations and diagnoses. A CAD system can support endoscopists in improving lesion detection rates, optimizing strategies during endoscopy for high-risk lesions, and increasing clinics' capacity while preserving diagnostic quality [8, 5].

Despite progress in machine learning and computer vision techniques, automatic polyp segmentation remains a difficult problem. Polyps are caused by abnormal cell growth in the human colon, meaning their appearances have strong relationships with the surroundings. Images of polyps come in a variety of shapes, sizes, textures, and colors. In addition, the boundary between polyps and their surrounding mucosa is not always clear during colonoscopy, especially in different lighting modes and in cases of flat lesions or unclean bowel preparation. These cause a lot of uncertainty for segmentation models.

The most widely used method for polyp segmentation in recent years is Convolution Neural Networks (CNNs). A majority of segmentation models use a UNet-based architecture containing an encoder and a decoder, both of which are CNNs. Despite being widely used for segmentation tasks with impressive performance, CNNs pose certain limitations: They can only capture local information while ignoring spatial context and global information; The dense connections make them computational expensive.

Transformer [46] is a more recent deep neural network architecture that models the global interactions among input components using attention mechanisms. While initially designed to tackle problems in natural language and speech processing, Transformers have had a significant impact on computer vision in recent years. Very recently, there has been fast-growing interest in using Transformers for semantic image segmentation [31, 48, 37, 55]. These methods use well-known encoder-decoder architectures wherein Transformers and CNNs are combined in various settings. The works in [31, 48, 37] proposed Transformer-CNN architectures, in which a Transformer is used as the encoder, and a traditional CNN is used as the decoder. Hybrid architectures of Transformers and CNN have been proposed in [55], in which the decoder is the traditional CNN or a Transformer, while the encoder is a combination of CNN and Transformer layers.

Inspired by these approaches for modeling multi-scale and multi-level features, we propose a new Transformers-based network called ColonFormer. The main design of our ColonFormer also contains a transformer encoder and a CNN decoder, but our approach is different from the above-mentioned models in several ways. In ColonFormer, the encoder is a hierarchically structured lightweight Transformer for learning multi-scale features. The decoder is a hierarchical pyramid structure with the capability of learning from heterogeneous data containing feature maps from encoder blocks at different scales and subregions. Besides, a refinement module is proposed for further improving the segmentation performance on hard regions and small polyps. Our main contributions include:

- A novel a deep neural network, ColonFormer, that integrates a hierarchical Transformer and a hierarchical pyramid CNN in a unified architecture for efficient and accurate polyp segmentation;
- A new refinement technique for feature fusion and smoothing aiming at improving the segmentation accuracy;
- A set of experiments on five standard benchmark datasets for polyp segmentation (Kvasir, CVC-Clinic DB, CVC-ColonDB, EndoScene, and ETIS) and comparisons of the effectiveness of ColonFormer to current state-of-the-art models.

2 Related Work

2.1 Convolution Neural Network

Convolutional Neural Network (CNN) is the most widely applied deep neural network architecture, especially in Computer Vision. A deep CNN extracts features on multiple layers with increasing levels of abstraction. Low-level features with high resolutions represent spatial details, while high-level features with low resolutions represent semantic information. CNNs are especially powerful in image processing as they are able to extract highly valuable and abstract features.

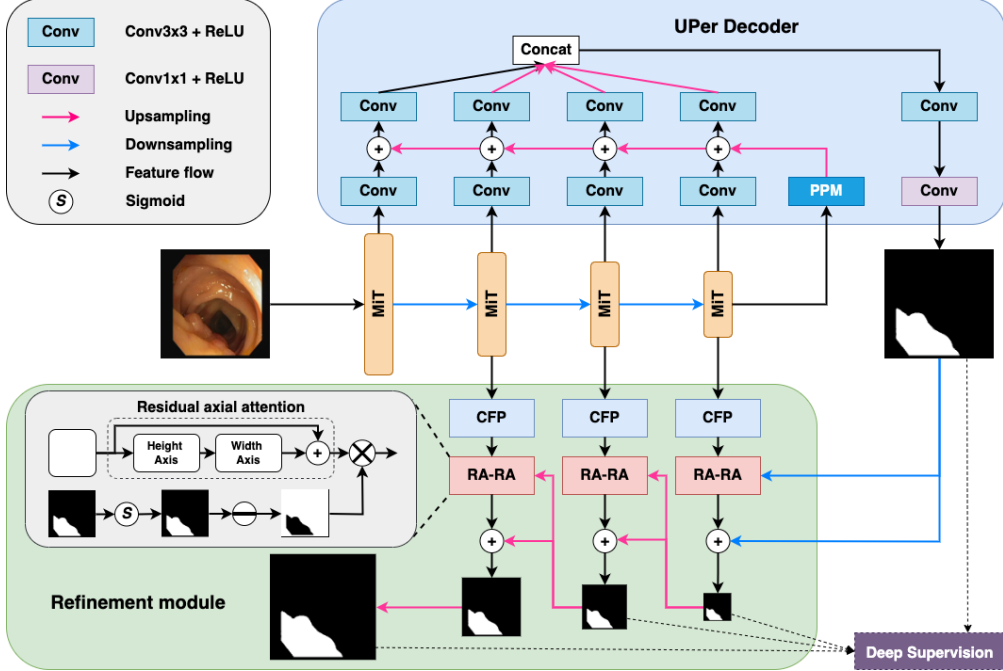


Figure 1: The overall architecture of our ColonFormer contains three components: an encoder, a decoder, and a refinement module. The encoder is based on the Mix Transformer backbone. The Uper Decoder starts with the Pyramid Pooling Module and then combines it with the output feature maps of the encoder at multi-levels to produce a global map. Finally, the refinement module gradually refines the boundary of the global map to yield the final accurate segmentation. Besides this final prediction, the global map and two intermediate maps are also passed into the training loss in a deep supervision manner. Before calculating the training loss, all refined maps are upsampled to the original image input size.

UNet [38] is a pioneering CNN architecture for medical image segmentation in general. UNet consists of an encoder and a decoder. The encoder includes convolutional, pooling layers for feature extraction, and the decoder uses up-sampling (or deconvolutional) and convolutional layers for reconstructing the final segmentation prediction. Later works further refined UNet by introducing skip connections, which alleviate information loss caused by stacking multiple convolution layers. However, retaining information may also introduce noisy signals that degrade performance. UNet variations such as UNet++ [57] and DoubleUnet [24] have achieved stellar results on segmentation benchmarks. UNet++ is constructed as an ensemble of nested UNets of varying depths, which partially share an encoder and jointly learn using deep supervision. DoubleUnet stacks two UNet blocks and uses ASPP [7] and SE blocks [17] to enhance the representation.

UNet encoders often use an existing pretrained architecture, also known as the backbone. Widely used backbones include VGG [42], MobileNet [16], ResNet [14], DenseNet [19], etc. PraNet [11] uses Res2Net as the backbone, while AG-CuResNeSt [39] uses ResNeSt. Meanwhile HarDNet-MSEG [18], NeoUNet [35] and BlazeNeo [1] use HarDNet, an improvement of DenseNet to extract features.

2.2 Attention Mechanism

Attention is a widely used technique to help deep neural networks create better feature representations, especially on highly variant inputs. Oktay et al. [40] proposed an Attention Gate module for UNet, which helps the model focus on necessary information while preserving computational efficiency. AG-ResUNet++ [20] integrates the attention gates with the ResNet backbone to improve UNet++ [57] for polyp segmentation. PraNet [11] uses the Reverse Attention mechanism [9], which enforces focus on the boundary between a polyp and its surroundings. In general, most CNNs and neural networks can benefit by adding attention modules. However, even with attention mechanisms, CNNs are limited by the locality of convolution operations. This makes it difficult for them to model natural long-range dependencies between input segments.

2.3 Vision Transformer

Transformer [46] is a highly influential deep neural network architecture, originally proposed to solve natural language processing and similar problems. While the original Transformer architecture is not very well suited for image processing, many works have been able to leverage its advantages for computer vision through some modifications. Vision Transformer (ViT) [27] was the first successful application of Transformer for computer vision. ViT splits an image into patches and processes them as sequential tokens. This method greatly reduces computational costs and allows Transformers to feasibly work with large images.

A major issue for ViT is that it requires very large datasets to remain effective while severely limited when trained on smaller datasets. Such property hinders its usage in problems such as polyp segmentation, where data is typically scarce. The Kvasir dataset, for example, contains just 1000 pictures and their corresponding ground truth, despite being the largest public dataset for polyp segmentation.

Later works have attempted to further enhance ViT in many ways. DeiT [45] introduces a data-efficient training strategy combined with a distillation approach, which helps improve performance on small datasets. On the other hand, the authors of Swin Transformer [31] redesigned the encoder for Transformers. The Swin Transformer encoder computes self-attention among a collection of adjacent patches within a sliding window. Patches are merged every few blocks, reducing the number of tokens and forming a multi-resolution token hierarchy similar to convolution blocks. SegFormer [52] is another hierarchical Transformer design, where patches are merged with overlap and preserving local continuity around patches. The authors also introduced Efficient Self-Attention, a modified attention mechanism for reducing computational complexity, and Mix-FFN for better positional information.

Both TransUNet [6] and TransFuse [53] have applied Transformers to polyp segmentation with positive results. TransUNet uses a Transformer-based network with a hybrid ViT encoder and upsampling CNN decoder. The Hybrid ViT stacks the CNN and Transformer together, leading to high computational costs. TransFuse addressed this problem by using a parallel architecture. Both models use the Attention Gate mechanism [40] and the BiFusion Module, which include SE Blocks [17] and CBAM Blocks [50]. These components make the network architecture large and highly complex.

While there have been promising results in applying Transformers to polyp segmentation, there is plenty of room for improvement in this direction. Most notably, reduced network size and latency can greatly benefit downstream applications. In addition, improved accuracy and robustness can also be achieved with more optimized architectures. In this paper, we seek to design a Transformer-based architecture that achieves these goals.

3 ColonFormer

Fig. 1 shows the overall architecture of our proposed network, called ColonFormer. ColonFormer consists of a hybrid encoder, a decoder, and a refinement module. We shall describe each component in detail in the following sections.

3.1 Encoder

A hierarchically structured model that can extract coarse to fine features at multi-scale and multi-level is desired for semantic segmentation. SegFormer uses Mix Transformer (MiT) [52] as the encoder backbone. MiT yields the multi-level resolution feature maps, which make our encoder become a hierarchical architecture. Assume $X \in \mathbf{R}^{H \times W \times C}$ denotes the input image. MiT generates the CNN-like multi-level features F_i . The hierarchical feature map F_i gets the resolution of $\frac{H}{2^{i+1}} \times \frac{W}{2^{i+1}} \times C_i$, where $i \in \{1, 2, 3, 4\}$ and C_i is ascending. The hierarchical feature representation is brought by the overlapped patch merging. After several Transformer blocks (Fig. 2a), a kernel with a stride smaller than kernel size is used to divide the feature map into patches. By striding the overlapped kernel, it can preserve the local continuity around those patches. Like the other Transformer blocks, MiT blocks contain three main parts: Multi-head Self-Attention (MHSA) layers, Feed Forward Network (FFN), and Layer Norm. The MHSA is improved into Efficient Self-Attention. By reducing the dimension of Keys in MHSA, it can save the computation cost. However, the point that we decide to choose MiT is the Mix-FFN. Instead of using the positional encoding (PE) as ViT, a 3×3 convolution kernel is integrated into FFN. Because the resolution of PE is fixed, it can not utilize the positional information of the pretrained dataset like ImageNet due to the resolution variance. Therefore, the PE needs to be interpolated, and that leads to a possible reduction in accuracy. By using convolution, a better position representation can be provided for Transformer. MiT has a series of models, from MiT-B0 to MiT-B5, which have the same architecture but different sizes. While conducting experiments, we found that MiT-B3 achieves the best results.

3.2 Decoder

In order to exploit global representations, feature maps from encoder blocks are first passed through a Pyramid Pooling Module (PPM) [54] before being processed by decoder blocks. A PPM simultaneously produces different scaled versions of the input feature map via a pyramid of pooling layers. The resulting feature maps form a hierarchy of features containing information at different scales and sub-regions, which are then concatenated to produce an efficient global prior representation. Fig. 2c depicts the Pyramid Pooling Module in detail.

ColonFormer uses a decoder architecture inspired by UPerNet [51], which we denote as UPer Decoder. The decoder uses convolution blocks on multiple image scales but fuses the output of the middle and low-level blocks instead of extracting the final high-level feature map. The fused feature map goes through several convolution layers to produce the final prediction mask.

3.3 Refinement Module

The decoder’s outputs are further processed by a refinement module to achieve more precise and complete prediction maps. The refinement module consists of Channel-wise Feature Pyramid (CFP) module [33] (Fig. 2b) and our novel Reverse Attention using Residual Axial Attention (RA-RA) for incremental correction of polyp boundary [9, 15].

Doctors in a clinical context initially find the polyp location roughly before carefully inspecting local tissues to precisely label the polyp. In PraNet, the global map is derived from the deepest CNN layer, so it does not have many structural details and hence can present only rough locations of the polyp tissues. According to the doctors, they proposed a strategy to mine complementary regions and details in a sequential manner by removing previously estimated polyp regions from high-level side-output features, where the current estimation is up-sampled from the deeper layer. By using Reverse Attention, a coarse saliency map is guided to sequentially discover complement object regions and details by erasing the current predicted salient regions from side-output features, where the current prediction is upsampled from its deeper layer. This erasing approach can refine the imprecise and coarse estimation into an accurate and complete prediction map. CaraNet [32] enhanced this strategy by integrating Reverse Attention with Axial Attention. Axial Attention is a simple generalization of self-attention that naturally aligns with the multiple dimensions of the tensors. This module selects the necessary information for refining progress by Reverse Attention. CaraNet also uses Channel-wise Feature Pyramid to extract features from the encoder in multi-scale views. Multi-scale features are fused gradually, which makes the final feature become more smooth. In our method, we apply the strategy of CaraNet but modify it by adding skip connections when integrating Axial Attention. We argue that the axial attention may not always be good for learning. Therefore, a residual connection can facilitate the learning process since it gives the model an option to omit the axial attention layers when needed. We evaluate the effectiveness of the novel refinement in Section 4.4.

3.4 Loss Function

ColonFormer uses Focal Loss and IoU loss during training. The loss function are computed as:

$$\mathcal{L}_{iou} = 1 - \frac{y * \hat{y}}{y + \hat{y} - y * \hat{y} + 1} \quad (1)$$

$$\mathcal{L}_{focal} = -\alpha(1 - BCE(y, \hat{y})^\gamma \log(BCE(y, \hat{y}))) \quad (2)$$

where y is the ground truth mask, \hat{y} is the prediction mask, α, γ are tunable hyperparameters and $BCE(y, \hat{y})$ is the binary cross-entropy loss of y and \hat{y} , which is defined as:

$$BCE(y, \hat{y}) = -(y \log(\hat{y}) + (1 - y) \log(1 - \hat{y})) \quad (3)$$

Furthermore, to focus the model on boundary regions, we use a per-pixel weighting scheme [49]. The weight for pixel (i, j) is calculated as:

$$\alpha_{ij} = \frac{\sum_{m,n \in A_{i,j}} g_{mn}}{\sum_{m,n \in A_{i,j}} 1} - g_{ij} \quad (4)$$

where g_{ij} is the ground truth value of pixel (i, j) , m and n are tunable hyperparameters that determine the size of the local region. α_{ij} estimate the importance of pixel (i, j) using difference between its own ground truth value and the surrounding pixels. A large value of α_{ij} indicates a pixel with considerable distinction from its surroundings, i.e., a pixel at a polyp’s border.

ColonFormer’s overall loss function is determined as:

$$\mathcal{L}_{total} = \frac{\mathcal{L}_{w focal} + \mathcal{L}_{w iou}}{2} \quad (5)$$

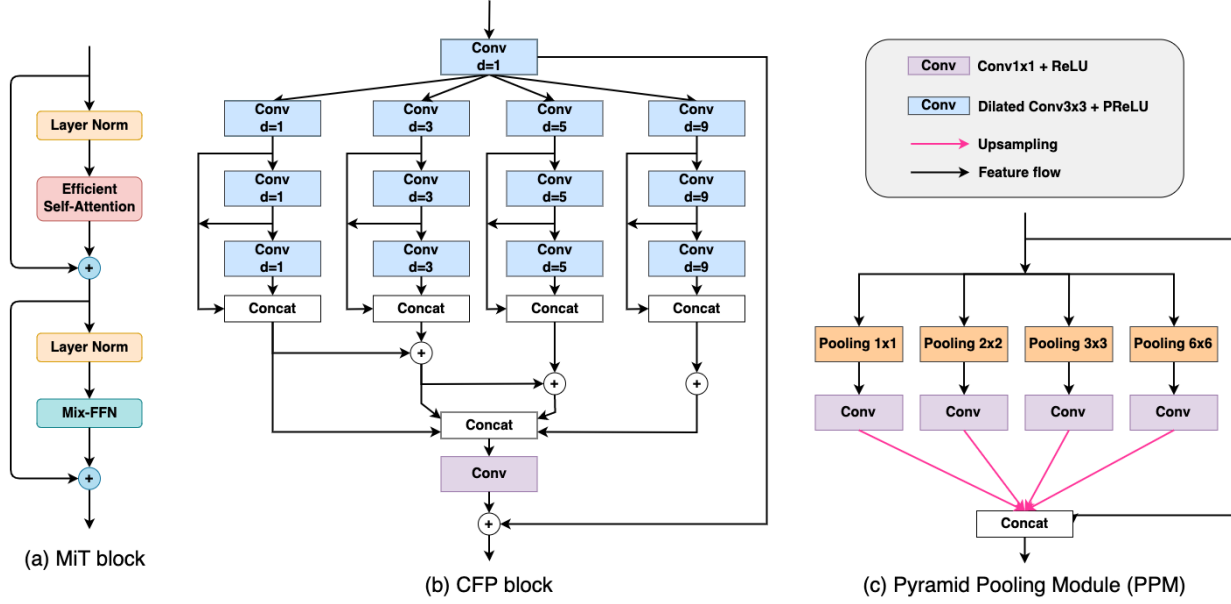


Figure 2: The architecture of three neural blocks used in our ColonFormer. The left block is the Mix Transformer block in Segformer [52]. The middle block is the channel-wise feature pyramid block with $d = 8$. The pyramid pooling module is shown on the right.

where \mathcal{L}_{wfocal} is the weighted focal loss, and \mathcal{L}_{wiou} is the weighted IoU loss.

$$\mathcal{L}_{wfocal} = -\frac{\sum_{i=1}^H \sum_{j=1}^W (1 + \gamma \alpha_{ij}) \sum_{l=0}^1 \mathbf{1}(g_{ij} = l) (1 - p_{ij})^\gamma \log(p_{ij})}{\sum_{i=1}^H \sum_{j=1}^W \gamma \alpha_{ij}} \quad (6)$$

$$\mathcal{L}_{wiou} = 1 - \frac{\sum_{i=1}^H \sum_{j=1}^W (g_{ij} * p_{ij}) * (1 + \gamma \alpha_{ij})}{\sum_{i=1}^H \sum_{j=1}^W (g_{ij} + p_{ij} - g_{ij} * p_{ij}) * (1 + \gamma \alpha_{ij})} \quad (7)$$

4 Experiments

4.1 Datasets

We perform experiments on the five largest datasets for polyp segmentation: Kvasir [25], CVC-Clinic DB [4], CVC-Colon DB [43], EndoScene [47] and ETIS-Larib Polyp DB [41]. Details of these datasets are described as follows:

- **Kvasir dataset (Kvasir):** The data is collected using endoscopic equipment at Vestre Viken Health Trust (VV), Norway. Images are carefully annotated and verified by experienced gastroenterologists from VV and the Cancer Registry of Norway (CRN). The dataset consists of 1000 images with different resolutions from 720x576 up to 1920x1072 pixels.
- **CVC-ClinicDB dataset (ClinicDB):** CVC-ClinicDB is a database of frames extracted from colonoscopy videos. The dataset consists of 612 images with a resolution of 384x288 pixels from 31 colonoscopy sequences. The dataset was used in the training stages of the MICCAI 2015 Sub-Challenge on Automatic Polyp Detection Challenge in Colonoscopy Videos.
- **CVC-ColonDB dataset (ColonDB):** CVC-ColonDB is provided by the Machine Vision Group (MVG). The dataset consists of 380 images with a resolution of 574x500 pixels from 15 short colonoscopy videos.
- **EndoScene dataset (EndoScene):** This dataset contains 612 images from the CVC-ClinicDB dataset and 300 images from the CVC-300 dataset in its training set. The test set, called CVC-T, consists of 60 images obtained from 44 video sequences acquired from 36 patients.
- **ETIS-Larib Polyp DB dataset (ETIS):** The ETIS-Larib Polyp DB dataset contains 196 high resolution (1226x996) colonoscopy images.

4.2 Experiment settings

We implement ColonFormer using the PyTorch framework. For the network backbone, as the original experiments [52], we use the same parameters as SegFormer [52]: kernel size $K = 7$, stride $S = 4$, padding size $P = 3$, and $K = 3, S = 2, P = 1$ to produce features with the same size as the non-overlapping process. Training is performed using Google Colaboratory, on virtual machines with 16GB RAM and an NVIDIA Tesla P100 GPU. Input images are resized to 352×352 for testing. During training, multiple image scales (0.75, 1, 1.25) are used to improve robustness. No other data augmentation method is performed during training.

ColonFormer employs the Adam optimization algorithm and cosine annealing scheduler with a learning rate of 1e-4 for parameter optimization. Models in our experiments are trained in 20 epochs with a batch size of 8. Each model is trained and evaluated five times and compared over their averaged results. We use six experiment setups to evaluate our method; each setup is described in detail below:

- **Experiment 1:** 5-fold cross-validation on the CVC-ClinicDB and Kvasir datasets, which is split into five equal folds. Each run uses one fold for testing and four folds for training.
- **Experiment 2:** Cross-dataset validation with 3 training-testing configurations:
 1. CVC-ColonDB and ETIS for training, CVC-ClinicDB for testing;
 2. CVC-ColonDB for training, CVC-ClinicDB for testing;
 3. CVC-ClinicDB for training, ETIS for testing.
- **Experiment 3:** Using 80% of the Kvasir and ClinicDB datasets for training and 10% for validation. The remaining images in the Kvasir and ClinicDB datasets, along with all data from ColonDB, EndoScene, and ETIS datasets, are used for testing.

The first experiment evaluates ColonFormer’s learning ability compared to several recent polyp segmentation. The second experiment provides deeper insights into the generalization capability of ColonFormer and other benchmark models. The third experiment compares ColonFormer with state-of-the-art CNN-based and Transformer-based networks (including PraNet [11], CaraNet [32], TransUNet [6] and TransFuse [53]) using a widely-used dataset configuration.

In addition, we perform a series of ablation studies to evaluate the effectiveness of each component in ColonFormer, namely:

- Investigating the effectiveness of the UPer Decoder
- Investigating the effectiveness of the Refinement Module
- Investigating the effectiveness of the Mix Transformer backbone

All ablation studies are performed on the dataset configuration for Experiment 3.

4.3 Comparison with benchmark models

Table 1 describes evaluation results in Experiment 1. For each metric, we measure both the average value and the standard deviation, which reflects model stability. ColonFormer outperforms all benchmark models in mDice, mIOU, and recall on both datasets. Notably, ColonFormer is the most stable model on both datasets, achieving the lowest standard deviation in every evaluation metric.

Qualitative results for Experiment 1 is shown in Fig. 4. ColonFormer shows much less noise in segmentation results compared to other models. ColonFormer also produces better ROC and PR curves than the benchmark models, as seen in Fig. 3.

Table 2 describes evaluation results for Experiment 2. Overall, ColonFormer significantly outperforms benchmark models on cross-dataset metrics. For the first configuration, ColonFormer outperforms the second-best PraNet by 7–8% on all metrics. In the second configuration, ColonFormer continues to achieve a 4.5% improvement in precision and 6.6% improvement in mDice over PraNet. Most notably, ColonFormer reports a 10% improvement in mDice and 18.3% in mDice over mDice in the third configuration. These are highly significant improvements, showing that ColonFormer can generalize very well to new data. Some result samples for this experiment are shown in Fig. 5.

Table 3 describes our evaluation results for Experiment 3. ColonFormer generally outperforms the benchmark models on most datasets. Notably, ColonFormer outperforms the second-best TransFuse-L* by 3% in mDice and 2.7% in mIOU on the ColonDB dataset. For the ETIS dataset, ColonFormer achieves an improvement of 5.4% in mDice and 5% in mIOU over the second-best CaraNet. However, ColonFormer also achieves roughly 1% lower metrics against TransFuse-L* on the ClinicDB dataset.

Table 1: Performance comparison of different methods on 5-fold cross-validation of the ClinicDB and Kvasir datasets. Metrics are averaged over 5 folds.

Dataset	Methods	mDice	mIOU	Recall	Precision
ClinicDB	UNet [38]	-	0.792	-	-
	MultiResUNet [21]	-	0.849	-	-
	ResUNet++ [26]	0.815 ± 0.018	0.736 ± 0.017	0.832 ± 0.018	0.830 ± 0.020
	DoubleUNet [24]	0.920 ± 0.018	0.866 ± 0.025	0.922 ± 0.027	0.928 ± 0.017
	DDANet [44]	0.860 ± 0.014	0.786 ± 0.017	0.858 ± 0.023	0.892 ± 0.014
	ColonSegNet [23]	0.817 ± 0.020	0.873 ± 0.024	0.926 ± 0.025	0.933 ± 0.014
	HarDNet-MSEG [18]	0.923 ± 0.020	0.873 ± 0.024	0.926 ± 0.025	0.933 ± 0.014
	PraNet [11]	0.933 ± 0.012	0.884 ± 0.015	0.940 ± 0.005	0.937 ± 0.016
Kvasir	ColonFormer (Ours)	0.947 ± 0.002	0.903 ± 0.003	0.956 ± 0.002	0.942 ± 0.005
	UNet [38]	0.708 ± 0.017	0.602 ± 0.010	0.805 ± 0.014	0.716 ± 0.020
	ResUNet++ [26]	0.780 ± 0.010	0.681 ± 0.008	0.834 ± 0.010	0.799 ± 0.010
	DoubleUNet [24]	0.879 ± 0.018	0.816 ± 0.026	0.902 ± 0.027	0.894 ± 0.039
	DDANet [44]	0.860 ± 0.005	0.791 ± 0.004	0.876 ± 0.015	0.892 ± 0.018
	ColonSegNet [23]	0.676 ± 0.037	0.557 ± 0.040	0.731 ± 0.088	0.730 ± 0.080
	HarDNet-MSEG [18]	0.889 ± 0.011	0.831 ± 0.011	0.892 ± 0.015	0.926 ± 0.014
	PraNet [11]	0.883 ± 0.020	0.822 ± 0.020	0.897 ± 0.020	0.906 ± 0.010
	ColonFormer (Ours)	0.917 ± 0.006	0.865 ± 0.007	0.932 ± 0.007	0.926 ± 0.008

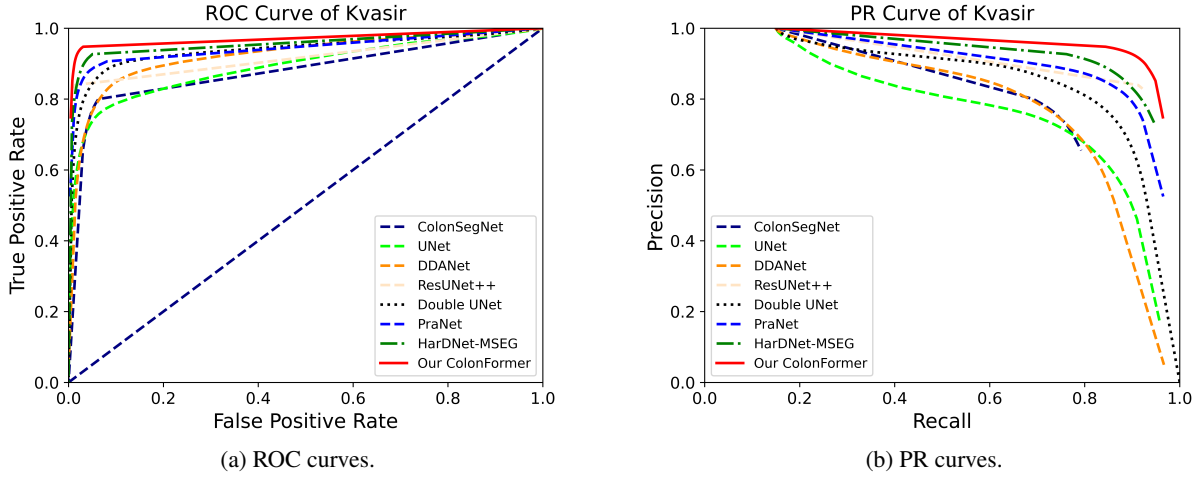


Figure 3: ROC curves and PR curves on the 5-fold cross-validation on the Kvasir-SEG dataset. All the curves are averaged over 5 folds.

Table 4 compares ColonFormer with other benchmark models in terms of size and computational complexity. Overall, ColonFormer remains larger than most CNN-based neural networks but more compact than Transformer-based methods.

4.4 Ablation studies

Effectiveness of the UPer Decoder. We firstly compare the original Segformer [52] with MLP Decoder and another model called Segformer-UPer that replaces the original MLP decoder with the UPer Decoder (ColonFormer-UPer). Results are shown in Table 5. Both network versions show similar metrics across the test datasets, with slight variations of roughly 1%. However, one can see from Table 4 that UPer Decoder is also significantly less costly, requiring only 20.99 GFLOPs as opposed to MLP Decoder (33.68 GFLOPs). These results compel us to choose the UPer decoder for ColonFormer, which alleviates the large computation costs incurred with the Transformer backbone.

Effectiveness of the Refinement Module. We evaluate the performance of Segformer-UPer-ARA with the Refinement Module as in [32], and our ColonFormer with the adjusted Refinement Module as described in Section 3.3. Results are shown in Table 5. Overall, incorporating the Refinement Module yields improvement across all datasets.

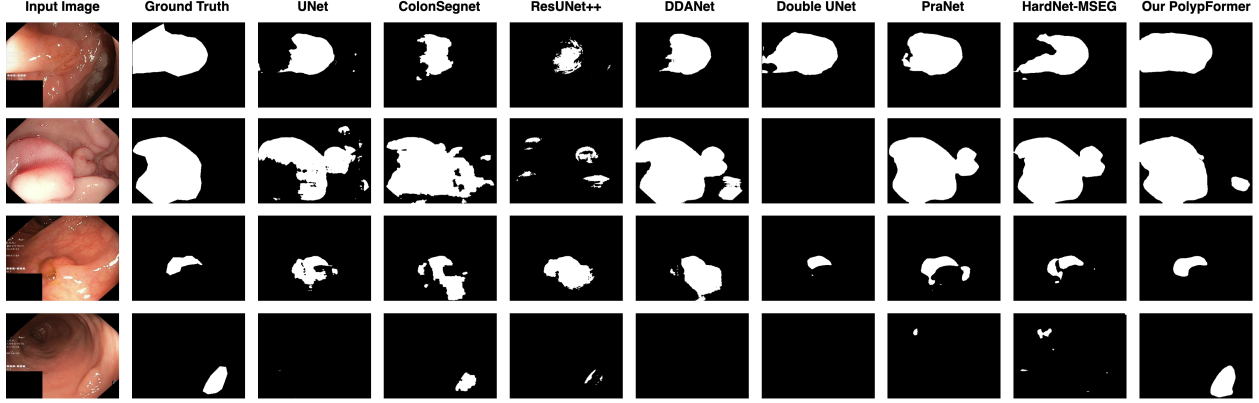


Figure 4: Qualitative result comparison of different models trained on the first fold of the 5-fold cross-validation on the Kvasir dataset.

Table 2: Performance comparison of different methods on cross-dataset configurations.

Trainset	Testset	Methods	mDice	mIOU	Recall	Precision
ColonDB+ETIS	ClinicDB	ResUNet++ [26]	0.406	0.302	0.481	0.496
		ColonSegNet [23]	0.427	0.321	0.529	0.552
		DDANet [44]	0.624	0.515	0.697	0.692
		DoubleUNet [24]	0.738	0.651	0.758	0.824
		HarDNet-MSEG [18]	0.765	0.681	0.774	0.863
		PraNet [11]	0.779	0.689	0.832	0.812
		<i>ColonFormer (Ours)</i>	0.847	0.770	0.844	0.902
ColonDB	ClinicDB	ResNet50-Mask-RCNN [36]	0.639	0.560	0.648	0.710
		ResNet101-Mask-RCNN [36]	0.641	0.565	0.646	0.725
		ResUNet++ [26]	0.339	0.247	0.380	0.484
		DoubleUNet [24]	0.441	0.375	0.423	0.639
		DDANet [44]	0.476	0.370	0.501	0.644
		ColonSegNet [23]	0.582	0.268	0.511	0.460
		HarDNet-MSEG [18]	0.721	0.633	0.744	0.818
		PraNet [11]	0.738	0.647	0.751	0.832
		<i>ColonFormer (Ours)</i>	0.804	0.723	0.794	0.877
ClinicDB	ETIS	ResNet50-Mask-RCNN [36]	0.501	0.412	0.546	0.573
		ResNet101-Mask-RCNN [36]	0.565	0.469	0.565	0.639
		DoubleUNet [24]	0.588	0.500	0.689	0.599
		ResUNet++ [26]	0.211	0.155	0.309	0.203
		ColonSegNet [23]	0.217	0.110	0.654	0.144
		DDANet [44]	0.400	0.313	0.507	0.464
		PraNet [11]	0.631	0.555	0.762	0.597
		HarDNet-MSEG [18]	0.659	0.583	0.676	0.705
		<i>ColonFormer (Ours)</i>	0.760	0.673	0.859	0.734

Our ColonFormer also yields superior performance than Segformer-Uper-ARA on the Kvasir, Clinic-DB and most significantly the ETIS datasets, while slightly underperforming on the ColonDB and EndoScene datasets.

Effectiveness of the MiT Backbone. The Mix Transformer (MiT) [52] backbone has several size variations ranging from MiT-B0 to MiT-B5. Table 6 shows our comparison of the ColonFormer architecture using each variation as the backbone. Overall, MiT-B3 yields the best results across our test datasets.

5 Conclusion

In this paper, we propose a hybrid CNN-Transformer architecture called ColonFormer to address the polyp segmentation problem. The proposed neural network aims to combine the strengths of both CNNs and Transformers while

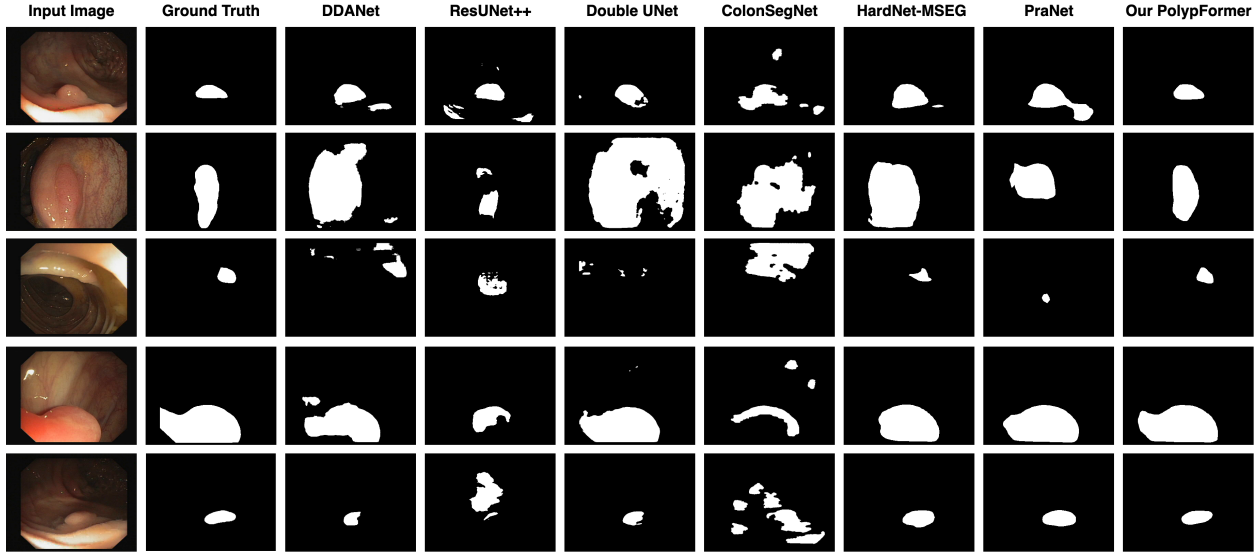


Figure 5: Qualitative result comparison using CVC-Colon for training and CVC-Clinic for testing.

Table 3: Performance comparison of different methods on the Kvasir, ClinicDB, ColonDB, EndoScene and ETIS test sets.

Methods	Kvasir		ClinicDB		ColonDB		CVC-T (EndoScene)		ETIS	
	mDice	mIOU	mDice	mIOU	mDice	mIOU	mDice	mIOU	mDice	mIOU
UNet [38]	0.818	0.746	0.823	0.750	0.512	0.444	0.710	0.627	0.398	0.335
UNet++ [57]	0.821	0.743	0.794	0.729	0.483	0.410	0.707	0.624	0.401	0.344
SFA [12]	0.723	0.611	0.700	0.607	0.469	0.347	0.297	0.217	0.467	0.329
PraNet [11]	0.898	0.840	0.899	0.849	0.709	0.640	0.871	0.797	0.628	0.567
HarDNet-MSEG [18]	0.912	0.857	0.932	0.882	0.731	0.660	0.887	0.821	0.677	0.613
CaraNet [32]	0.918	0.865	0.936	0.887	0.773	0.689	0.903	0.838	0.747	0.672
TransUNet [6]	0.913	0.857	0.935	0.887	0.781	0.699	0.893	0.824	0.731	0.660
TransFuse-L* [53]	0.920	0.870	0.942	0.897	0.781	0.706	0.894	0.826	0.737	0.663
<i>ColonFormer (Ours)</i>	0.924	0.876	0.932	0.884	0.811	0.733	0.906	0.842	0.801	0.722

Table 4: Number of parameters and GFLOPs of different methods

Methods	Parameters (M)	GFLOPs
PraNet [11]	32.55	13.11
HarDNet-MSEG [18]	33.34	11.38
CaraNet [32]	46.64	21.69
TransUNet [6]	105.5	60.75
TransFuse-L* [53]	-	-
Segformer [52]	47.22	33.68
Segformer-Uper (MiT + Uper decoder)	46.61	20.99
<i>ColonFormer (Ours)</i>	52.94	22.94

adapting to the various challenges of segmenting polyps in medical images. Our extensive experiments show that ColonFormer significantly outperforms current state-of-the-art models on benchmark datasets.

6 Acknowledgments

This work was funded by Vingroup Innovation Foundation (VINIF) under project code VINIF.2020.DA17.

Table 5: Ablation study on the effectiveness of different components when they are integrated with the original Segformer [52] using MiT backbone and MLP decoder

Method	Uper	A-RA	RA-RA	Kvasir		ClinicDB		ColonDB		EndoScene		ETIS	
				mDice	mIOU								
Segformer [52]	—	—	—	0.920	0.866	0.925	0.876	0.806	0.726	0.905	0.840	0.786	0.707
Segformer-Uper	✓	—	—	0.921	0.869	0.928	0.881	0.795	0.718	0.904	0.838	0.782	0.704
Segformer-Uper-ARA	✓	✓	—	0.921	0.871	0.928	0.881	0.815	0.737	0.912	0.848	0.787	0.708
<i>ColonFormer (Ours)</i>	✓	—	✓	0.924	0.876	0.932	0.884	0.811	0.733	0.906	0.842	0.801	0.722

Table 6: Evaluation metrics for ColonFormer-MiT-B1, ColonFormer-MiT-B2, ColonFormer-MiT-B3, ColonFormer-MiT-B4 and ColonFormer-MiT-B5

Methods	Kvasir		ClinicDB		ColonDB		EndoScene		ETIS	
	mDice	mIOU								
ColonFormer-MiT-B1	0.895	0.836	0.918	0.868	0.772	0.686	0.873	0.798	0.698	0.624
ColonFormer-MiT-B2	0.911	0.860	0.925	0.875	0.805	0.724	0.891	0.823	0.771	0.695
ColonFormer-MiT-B3	0.924	0.876	0.932	0.884	0.811	0.733	0.906	0.842	0.801	0.722
ColonFormer-MiT-B4	0.922	0.874	0.931	0.883	0.802	0.725	0.909	0.844	0.784	0.705
ColonFormer-MiT-B5	0.917	0.867	0.929	0.880	0.805	0.728	0.909	0.842	0.784	0.706

References

- [1] Nguyen S An, Phan N Lan, Dao V Hang, Dao V Long, Tran Q Trung, Nguyen T Thuy, and Dinh V Sang. Blazeneo: Blazing fast polyp segmentation and neoplasm detection. *IEEE Access*, 2022.
- [2] Mohammad Ali Armin, Hans De Visser, Girija Chetty, Cedric Dumas, David Conlan, Florian Grimpenn, and Olivier Salvado. Visibility map: a new method in evaluation quality of optical colonoscopy. In *International Conference on Medical Image Computing and Computer-Assisted Intervention*, pages 396–404. Springer, 2015.
- [3] J. Bernal, N. Tajkbaksh, F. J. Sánchez, B. J. Matuszewski, H. Chen, L. Yu, Q. Angermann, O. Romain, B. Rustad, I. Balasingham, K. Pogorelov, S. Choi, Q. Debard, L. Maier-Hein, S. Speidel, D. Stoyanov, P. Brandao, H. Córdova, C. Sánchez-Montes, S. R. Gurudu, G. Fernández-Esparrach, X. Dray, J. Liang, and A. Histace. Comparative validation of polyp detection methods in video colonoscopy: Results from the miccai 2015 endoscopic vision challenge. *IEEE Transactions on Medical Imaging*, 36(6):1231–1249, 2017.
- [4] Jorge Bernal, F Javier Sánchez, Gloria Fernández-Esparrach, Debora Gil, Cristina Rodríguez, and Fernando Vilariño. Wm-dova maps for accurate polyp highlighting in colonoscopy: Validation vs. saliency maps from physicians. *Computerized Medical Imaging and Graphics*, 43:99–111, 2015.
- [5] Raf Bisschops, James E East, Cesare Hassan, Yark Hazewinkel, Michał F Kamiński, Helmut Neumann, Maria Pellisé, Giulio Antonelli, Marco Bustamante Balen, Emmanuel Coron, et al. Advanced imaging for detection and differentiation of colorectal neoplasia: European society of gastrointestinal endoscopy (esge) guideline—update 2019. *Endoscopy*, 51(12):1155–1179, 2019.
- [6] Jieneng Chen, Yongyi Lu, Qihang Yu, Xiangde Luo, Ehsan Adeli, Yan Wang, Le Lu, Alan L Yuille, and Yuyin Zhou. Transunet: Transformers make strong encoders for medical image segmentation. *arXiv preprint arXiv:2102.04306*, 2021.
- [7] Liang-Chieh Chen, George Papandreou, Iasonas Kokkinos, Kevin Murphy, and Alan L Yuille. Deeplab: Semantic image segmentation with deep convolutional nets, atrous convolution, and fully connected crfs. *IEEE transactions on pattern analysis and machine intelligence*, 40(4):834–848, 2017.
- [8] Peng-Jen Chen, Meng-Chiung Lin, Mei-Ju Lai, Jung-Chun Lin, Henry Horng-Shing Lu, and Vincent S Tseng. Accurate classification of diminutive colorectal polyps using computer-aided analysis. *Gastroenterology*, 154(3):568–575, 2018.
- [9] Shuhan Chen, Xiuli Tan, Ben Wang, and Xuelong Hu. Reverse attention for salient object detection. In *Proceedings of the European conference on computer vision (ECCV)*, pages 234–250, 2018.
- [10] Douglas A Corley, Christopher D Jensen, Amy R Marks, Wei K Zhao, Jeffrey K Lee, Chyke A Doubeni, Ann G Zauber, Jolanda de Boer, Bruce H Fireman, Joanne E Schottinger, et al. Adenoma detection rate and risk of colorectal cancer and death. *New england journal of medicine*, 370(14):1298–1306, 2014.
- [11] Deng-Ping Fan, Ge-Peng Ji, Tao Zhou, Geng Chen, Huazhu Fu, Jianbing Shen, and Ling Shao. Planet: Parallel reverse attention network for polyp segmentation. In *International Conference on Medical Image Computing and Computer-Assisted Intervention*, pages 263–273. Springer, 2020.

[12] Yuqi Fang, Cheng Chen, Yixuan Yuan, and Kai-yu Tong. Selective feature aggregation network with area-boundary constraints for polyp segmentation. In *International Conference on Medical Image Computing and Computer-Assisted Intervention*, pages 302–310. Springer, 2019.

[13] Michael Gschwantler, Stephan Kriwanek, Erich Langner, Bernhard Göritzer, Christiane Schrutka-Kölbl, Eva Brownstone, Hans Feichtinger, and Werner Weiss. High-grade dysplasia and invasive carcinoma in colorectal adenomas: a multivariate analysis of the impact of adenoma and patient characteristics. *European journal of gastroenterology & hepatology*, 14(2):183–188, 2002.

[14] Kaiming He, Xiangyu Zhang, Shaoqing Ren, and Jian Sun. Deep residual learning for image recognition. In *Proceedings of the IEEE conference on computer vision and pattern recognition*, pages 770–778, 2016.

[15] Jonathan Ho, Nal Kalchbrenner, Dirk Weissenborn, and Tim Salimans. Axial attention in multidimensional transformers. *arXiv preprint arXiv:1912.12180*, 2019.

[16] Andrew G Howard, Menglong Zhu, Bo Chen, Dmitry Kalenichenko, Weijun Wang, Tobias Weyand, Marco Andreetto, and Hartwig Adam. Mobilenets: Efficient convolutional neural networks for mobile vision applications. *arXiv preprint arXiv:1704.04861*, 2017.

[17] Jie Hu, Li Shen, and Gang Sun. Squeeze-and-excitation networks. In *Proceedings of the IEEE conference on computer vision and pattern recognition*, pages 7132–7141, 2018.

[18] Chien-Hsiang Huang, Hung-Yu Wu, and Youn-Long Lin. Hardnet-mseg: A simple encoder-decoder polyp segmentation neural network that achieves over 0.9 mean dice and 86 fps. *arXiv preprint arXiv:2101.07172*, 2021.

[19] Gao Huang, Zhuang Liu, Laurens Van Der Maaten, and Kilian Q Weinberger. Densely connected convolutional networks. In *Proceedings of the IEEE conference on computer vision and pattern recognition*, pages 4700–4708, 2017.

[20] Nguyen Ba Hung, Nguyen Thanh Duc, Thai Van Chien, and Dinh Viet Sang. Ag-resunet++: An improved encoder-decoder based method for polyp segmentation in colonoscopy images. In *2021 RIVF International Conference on Computing and Communication Technologies (RIVF)*, pages 1–6. IEEE, 2021.

[21] Nabil Ibtehaz and M Sohel Rahman. Multiresunet: Rethinking the u-net architecture for multimodal biomedical image segmentation. *Neural Networks*, 121:74–87, 2020.

[22] Iyad A Issa and Malak Noureddine. Colorectal cancer screening: An updated review of the available options. *World journal of gastroenterology*, 23(28):5086, 2017.

[23] Debesh Jha, Sharib Ali, Nikhil Kumar Tomar, Håvard D Johansen, Dag Johansen, Jens Rittscher, Michael A Riegler, and Pål Halvorsen. Real-time polyp detection, localization and segmentation in colonoscopy using deep learning. *Ieee Access*, 9:40496–40510, 2021.

[24] Debesh Jha, Michael A Riegler, Dag Johansen, Pål Halvorsen, and Håvard D Johansen. Doubleu-net: A deep convolutional neural network for medical image segmentation. In *2020 IEEE 33rd International symposium on computer-based medical systems (CBMS)*, pages 558–564. IEEE, 2020.

[25] Debesh Jha, Pia H Smedsrød, Michael A Riegler, Pål Halvorsen, Thomas de Lange, Dag Johansen, and Håvard D Johansen. Kvasir-seg: A segmented polyp dataset. In *International Conference on Multimedia Modeling*, pages 451–462. Springer, 2020.

[26] Debesh Jha, Pia H Smedsrød, Michael A Riegler, Dag Johansen, Thomas De Lange, Pål Halvorsen, and Håvard D Johansen. Resunet++: An advanced architecture for medical image segmentation. In *2019 IEEE International Symposium on Multimedia (ISM)*, pages 225–2255. IEEE, 2019.

[27] Alexander Kolesnikov, Alexey Dosovitskiy, Dirk Weissenborn, Georg Heigold, Jakob Uszkoreit, Lucas Beyer, Matthias Minderer, Mostafa Dehghani, Neil Houlsby, Sylvain Gelly, Thomas Unterthiner, and Xiaohua Zhai. An image is worth 16x16 words: Transformers for image recognition at scale. In *9th International Conference on Learning Representations, ICLR 2021, Virtual Event, Austria, May 3-7, 2021*, 2021.

[28] Shin-ei Kudo, Yuichi Mori, Masashi Misawa, Kenichi Takeda, Toyoki Kudo, Hayato Itoh, Masahiro Oda, and Kensaku Mori. Artificial intelligence and colonoscopy: Current status and future perspectives. *Digestive Endoscopy*, 31(4):363–371, 2019.

[29] Suck-Ho Lee, Il-Kwun Chung, Sun-Joo Kim, Jin-Oh Kim, Bong-Min Ko, Young Hwangbo, Won Ho Kim, Dong Hun Park, Sang Kil Lee, Cheol Hee Park, et al. An adequate level of training for technical competence in screening and diagnostic colonoscopy: a prospective multicenter evaluation of the learning curve. *Gastrointestinal endoscopy*, 67(4):683–689, 2008.

[30] AM Leufkens, MGH Van Oijen, FP Vleggaar, and PD Siersema. Factors influencing the miss rate of polyps in a back-to-back colonoscopy study. *Endoscopy*, 44(05):470–475, 2012.

[31] Ze Liu, Yutong Lin, Yue Cao, Han Hu, Yixuan Wei, Zheng Zhang, Stephen Lin, and Baining Guo. Swin transformer: Hierarchical vision transformer using shifted windows. In *Proceedings of the IEEE/CVF International Conference on Computer Vision*, pages 10012–10022, 2021.

[32] Ange Lou, Shuyue Guan, and Murray Loew. Caranet: Context axial reverse attention network for segmentation of small medical objects. *arXiv preprint arXiv:2108.07368*, 2021.

[33] Ange Lou and Murray Loew. Cfpnet: channel-wise feature pyramid for real-time semantic segmentation. In *2021 IEEE International Conference on Image Processing (ICIP)*, pages 1894–1898. IEEE, 2021.

[34] Pablo Mesejo, Daniel Pizarro, Armand Abergel, Olivier Rouquette, Sylvain Beorchia, Laurent Poincloux, and Adrien Bartoli. Computer-aided classification of gastrointestinal lesions in regular colonoscopy. *IEEE transactions on medical imaging*, 35(9):2051–2063, 2016.

[35] Phan Ngoc Lan, Nguyen Sy An, Dao Viet Hang, Dao Van Long, Tran Quang Trung, Nguyen Thi Thuy, and Dinh Viet Sang. Neounet: Towards accurate colon polyp segmentation and neoplasm detection. In *International Symposium on Visual Computing*, pages 15–28. Springer, 2021.

[36] Hemin Ali Qadir, Younghak Shin, Johannes Solhusvik, Jacob Bergsland, Lars Aabakken, and Ilangko Balasingham. Polyp detection and segmentation using mask r-cnn: Does a deeper feature extractor cnn always perform better? In *2019 13th International Symposium on Medical Information and Communication Technology (ISMIC-T)*, pages 1–6. IEEE, 2019.

[37] René Ranftl, Alexey Bochkovskiy, and Vladlen Koltun. Vision transformers for dense prediction. In *Proceedings of the IEEE/CVF International Conference on Computer Vision*, pages 12179–12188, 2021.

[38] Olaf Ronneberger, Philipp Fischer, and Thomas Brox. U-net: Convolutional networks for biomedical image segmentation. In *International Conference on Medical image computing and computer-assisted intervention*, pages 234–241. Springer, 2015.

[39] Dinh Viet Sang, Tran Quang Chung, Phan Ngoc Lan, Dao Viet Hang, Dao Van Long, and Nguyen Thi Thuy. Ag-curesnest: A novel method for colon polyp segmentation. *arXiv preprint arXiv:2105.00402*, 2021.

[40] Jo Schlemper, Ozan Oktay, Michiel Schaap, Matthias Heinrich, Bernhard Kainz, Ben Glocker, and Daniel Rueckert. Attention gated networks: Learning to leverage salient regions in medical images. *Medical image analysis*, 53:197–207, 2019.

[41] Juan Silva, Aymeric Histace, Olivier Romain, Xavier Dray, and Bertrand Granado. Toward embedded detection of polyps in wce images for early diagnosis of colorectal cancer. *International journal of computer assisted radiology and surgery*, 9(2):283–293, 2014.

[42] Karen Simonyan and Andrew Zisserman. Very deep convolutional networks for large-scale image recognition. *arXiv preprint arXiv:1409.1556*, 2014.

[43] Nima Tajbakhsh, Suryakanth R Gurudu, and Jianming Liang. Automated polyp detection in colonoscopy videos using shape and context information. *IEEE transactions on medical imaging*, 35(2):630–644, 2015.

[44] Nikhil Kumar Tomar, Debesh Jha, Sharib Ali, Håvard D Johansen, Dag Johansen, Michael A Riegler, and Pål Halvorsen. Ddanet: Dual decoder attention network for automatic polyp segmentation. In *ICPR International Workshop and Challenges*, 2021.

[45] Hugo Touvron, Matthieu Cord, Matthijs Douze, Francisco Massa, Alexandre Sablayrolles, and Hervé Jégou. Training data-efficient image transformers & distillation through attention. In *International Conference on Machine Learning*, pages 10347–10357. PMLR, 2021.

[46] Ashish Vaswani, Noam Shazeer, Niki Parmar, Jakob Uszkoreit, Llion Jones, Aidan N Gomez, Łukasz Kaiser, and Illia Polosukhin. Attention is all you need. *Advances in neural information processing systems*, 30, 2017.

[47] David Vázquez, Jorge Bernal, F Javier Sánchez, Gloria Fernández-Esparrach, Antonio M López, Adriana Romero, Michal Drozdzal, and Aaron Courville. A benchmark for endoluminal scene segmentation of colonoscopy images. *Journal of healthcare engineering*, 2017, 2017.

[48] Wenhui Wang, Enze Xie, Xiang Li, Deng-Ping Fan, Kaitao Song, Ding Liang, Tong Lu, Ping Luo, and Ling Shao. Pyramid vision transformer: A versatile backbone for dense prediction without convolutions. In *Proceedings of the IEEE/CVF International Conference on Computer Vision*, pages 568–578, 2021.

[49] Jun Wei, Shuhui Wang, and Qingming Huang. F³net: Fusion, feedback and focus for salient object detection. In *Proceedings of the AAAI Conference on Artificial Intelligence*, volume 34, pages 12321–12328, 2020.

[50] Sanghyun Woo, Jongchan Park, Joon-Young Lee, and In So Kweon. Cbam: Convolutional block attention module. In *Proceedings of the European conference on computer vision (ECCV)*, pages 3–19, 2018.

- [51] Tete Xiao, Yingcheng Liu, Bolei Zhou, Yuning Jiang, and Jian Sun. Unified perceptual parsing for scene understanding. In *Proceedings of the European Conference on Computer Vision (ECCV)*, pages 418–434, 2018.
- [52] Enze Xie, Wenhui Wang, Zhiding Yu, Anima Anandkumar, Jose M Alvarez, and Ping Luo. Segformer: Simple and efficient design for semantic segmentation with transformers. *Advances in Neural Information Processing Systems*, 34, 2021.
- [53] Yundong Zhang, Huiye Liu, and Qiang Hu. Transfuse: Fusing transformers and cnns for medical image segmentation. In *International Conference on Medical Image Computing and Computer-Assisted Intervention*, pages 14–24. Springer, 2021.
- [54] Hengshuang Zhao, Jianping Shi, Xiaojuan Qi, Xiaogang Wang, and Jiaya Jia. Pyramid scene parsing network. In *Proceedings of the IEEE conference on computer vision and pattern recognition*, pages 2881–2890, 2017.
- [55] Sixiao Zheng, Jiachen Lu, Hengshuang Zhao, Xiatian Zhu, Zekun Luo, Yabiao Wang, Yanwei Fu, Jianfeng Feng, Tao Xiang, Philip HS Torr, et al. Rethinking semantic segmentation from a sequence-to-sequence perspective with transformers. In *Proceedings of the IEEE/CVF conference on computer vision and pattern recognition*, pages 6881–6890, 2021.
- [56] Guanyu Zhou, Xiaogang Liu, Tyler M Berzin, Jeremy R Glissen Brown, Liangping Li, Chao Zhou, Zhenzhen Guo, Lei Lei, Fei Xiong, Yan Pan, et al. 951e—a real-time automatic deep learning polyp detection system increases polyp and adenoma detection during colonoscopy: a prospective double-blind randomized study. *Gastroenterology*, 156(6):S–1511, 2019.
- [57] Zongwei Zhou, Md Mahfuzur Rahman Siddiquee, Nima Tajbakhsh, and Jianming Liang. Unet++: A nested u-net architecture for medical image segmentation. In *Deep learning in medical image analysis and multimodal learning for clinical decision support*, pages 3–11. Springer, 2018.